

## Nanosecond CO Photodissociation and Excited-State Character of [Ru(X)(X')(CO)<sub>2</sub>(N,N'-diisopropyl-1,4-diazabutadiene)] (X = X' = Cl or I; X = Me, X' = I; X = SnPh<sub>3</sub>, X' = Cl) Studied by Time-Resolved Infrared Spectroscopy and DFT Calculations

Anders Gabrielsson,<sup>†</sup> Mike Towrie,<sup>‡</sup> Stanislav Zálaiš,<sup>§</sup> and Antonín Vlček, Jr.<sup>\*,†,§</sup>

School of Biological and Chemical Sciences, Queen Mary, University of London, Mile End Road, London E1 4NS, United Kingdom, Central Laser Facility, Science & Technology Facilities Council, Rutherford Appleton Laboratory, Didcot, Oxfordshire OX11 0QX, United Kingdom, and J. Heyrovský Institute of Physical Chemistry, Academy of Sciences of the Czech Republic, Dolejškova 3, CZ-182 23 Prague, Czech Republic

Received November 22, 2007

The character and dynamics of the low-lying excited states of [Ru(X)(X')(CO)<sub>2</sub>(iPr-dab)] (X = X' = Cl or I; X = Me, X' = I; X = SnPh<sub>3</sub>, X' = Cl; iPr-dab = N,N'-diisopropyl-1,4-diazabutadiene) were studied experimentally by pico- and nanosecond time-resolved IR spectroscopy (TRIR) and (for X = X' = Cl or I) computationally using density functional theory (DFT) and time-dependent DFT (TD-DFT) techniques. The lowest allowed electronic transition occurs between 390 and 460 nm and involves charge transfer from the Ru(halide)(CO)<sub>2</sub> unit to iPr-dab, denoted <sup>1</sup>MLCT/XLCT (metal-to-ligand/halide-to-ligand charge transfer). The lowest triplet state is well modeled by UKS-DFT-CPCM calculations, which quite accurately reproduce the excited-state IR spectrum in the  $\nu(\text{CO})$  region. It has a <sup>3</sup>MLCT/XLCT character with an intraligand (iPr-dab) <sup>3</sup> $\pi\pi^*$  admixture. TRIR spectra of the lowest triplet excited state show two  $\nu(\text{CO})$  bands that are shifted to higher energies from their corresponding ground-state positions. The magnitude of this upward shift increases as a function of the ligands X and X' [(I)<sub>2</sub> < (Sn)(Cl) < (Me)(I) < (Cl)<sub>2</sub>] and reveals increasing contribution of the Ru(CO)<sub>2</sub> → dab MLCT character to the excited state. The lowest triplet state of [Ru(Cl)<sub>2</sub>(CO)<sub>2</sub>(iPr-dab)] undergoes a ~10 ps relaxation that is followed by CO dissociation, producing *cis*(CO,CH<sub>3</sub>CN),*trans*(Cl,Cl)-[Ru(Cl)<sub>2</sub>(CH<sub>3</sub>CN)(CO)(iPr-dab)] with a unity quantum yield and 7.2 ns lifetime and without any observable intermediate. To our knowledge, this is the first example of a “slow” CO dissociation from a thermally equilibrated triplet charge-transfer excited state.

### Introduction

There is an ever-increasing demand for new chromophores and luminophores for photonic devices, photosensitizers, radical initiators, or light-harvesting applications. Ruthenium carbonyldiimine complexes of the type [Ru(X)(X')(CO)<sub>2</sub>( $\alpha$ -diimine)] constitute an important group of chromophores and catalysts, with diverse photochemistry and photophysics.<sup>1–4</sup>

Depending on the nature of the X and X' ligands and the  $\alpha$ -diimine, their excited states can be long-lived, emissive, and unreactive,<sup>5–8</sup> can undergo homolysis of Ru–X bonds

\* To whom correspondence should be addressed. E-mail: a.vlcek@qmul.ac.uk.

<sup>†</sup> University of London.

<sup>‡</sup> Rutherford Appleton Laboratory.

<sup>§</sup> Academy of Sciences of the Czech Republic.

(1) Stufkens, D. J.; Aarnts, M. P.; Rossenaar, B. D.; Vlček, A., Jr. *Pure Appl. Chem.* **1997**, *69*, 831.

(2) Stufkens, D. J.; Vlček, A., Jr. *Coord. Chem. Rev.* **1998**, *177*, 127.

(3) Stufkens, D. J.; Aarnts, M. P.; Nijhoff, J.; Rossenaar, B. D.; Vlček, A., Jr. *Coord. Chem. Rev.* **1998**, *171*, 93.

(4) van Slageren, J.; Hartl, F.; Stufkens, D. J.; Martino, D. M.; van Willigen, H. *Coord. Chem. Rev.* **2000**, *208*, 309.

(5) Aarnts, M. P.; Stufkens, D. J.; Vlček, A., Jr. *Inorg. Chim. Acta* **1997**, *266*, 37.

(6) Nieuwenhuis, H. A.; Stufkens, D. J.; Oskam, A.; Vlček, A., Jr. *Inorg. Chem.* **1995**, *34*, 3879.

(7) Nieuwenhuis, H. A.; Stufkens, D. J.; McNicholl, R.-A.; Al-Obaidi, A. H. R.; Coates, C. G.; Bell, S. E. J.; McGarvey, J. J.; Westwell, J.; George, M. W.; Turner, J. J. *J. Am. Chem. Soc.* **1995**, *117*, 5579.

(8) Nieuwenhuis, H. A.; Stufkens, D. J.; Oskam, A. *Inorg. Chem.* **1994**, *33*, 3212.

producing radicals,<sup>5,6,9–11</sup> or can lose CO,<sup>12–15</sup> leading to coordinatively unsaturated species, which have been studied<sup>16–18</sup> in relation to a catalytic water-gas shift reaction or CO<sub>2</sub> reduction and can undergo interesting structural reorganization and isomerization reactions.<sup>10,15</sup>

Photochemical CO dissociation from [Ru(X)(X')(CO)<sub>2</sub>(α-diimine)] is very interesting mechanistically. It presents a rare case of dissociation of an equatorial CO ligand, which lies in the Ru(diimine) plane. In contrast, in the case of metal tri- or tetracarbonyldiimine complexes,<sup>19,20</sup> it is always the axial CO ligand that dissociates. Recently, we have studied the mechanism of the photochemistry of *cis*(CO,CO),*trans*(X,X)-[Ru(X)<sub>2</sub>(CO)<sub>2</sub>(bpy)] (X = Cl, Br, I), whose stationary irradiation leads to dissociative isomerization, producing *cis*(CO,Solv),*cis*(X,X)-[Ru(X)<sub>2</sub>(Solv)(CO)(bpy)].<sup>12–14,21,22</sup> Using time-resolved IR spectroscopy (TRIR) spectra, we have shown<sup>15</sup> that, for X = Cl or Br, the CO dissociation is an ultrafast process that is followed by a 13–15 ps rearrangement to the *cis*(X,X) isomer. Essentially the same mechanism, but with a parallel population of a lower-lying unreactive triplet state, operates for X = I. Ultrafast CO dissociation coupled with structural reorganization was found also for analogous [Ru(I)<sub>2</sub>(CO)<sub>2</sub>(dcbpy)] (dcbpy = 4,4'-dicarboxy-2,2'-bipyridine).<sup>23,24</sup>

Herein, we have investigated photochemical CO dissociation from *cis*(CO,CO),*trans*(Cl,Cl)-[Ru(Cl)<sub>2</sub>(CO)<sub>2</sub>(iPr-dab)] (Figure 1) using pico- and nanosecond TRIR. For comparison, we have also studied picosecond TRIR spectra of analogous complexes [Ru(I)<sub>2</sub>(CO)<sub>2</sub>(iPr-dab)]<sup>25</sup> and the photostable<sup>5,6,8–10,26</sup> [Ru(Me)(I)(CO)<sub>2</sub>(iPr-dab)] and [Ru(SnPh<sub>3</sub>)(Cl)(CO)<sub>2</sub>(iPr-dab)], characterizing their lowest excited states.

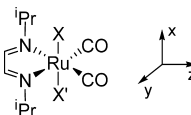


**Figure 1.** Schematic structure of the investigated complexes *cis*(CO,CO),*trans*(X,X')-[Ru(SnPh<sub>3</sub>)(Cl)(CO)<sub>2</sub>(iPr-dab)], [Ru(CH<sub>3</sub>)(I)(CO)<sub>2</sub>(iPr-dab)], [Ru(I)<sub>2</sub>(CO)<sub>2</sub>(iPr-dab)], and [Ru(Cl)<sub>2</sub>(CO)<sub>2</sub>(iPr-dab)], shown with the chosen orientation of axes. Hereinafter, the prefix *cis*(CO,CO),*trans*(X,X') is omitted for brevity.

Stationary irradiation of [Ru(Cl)<sub>2</sub>(CO)<sub>2</sub>(iPr-dab)] leads to straight CO photosubstitution by a solvent molecule.<sup>18</sup> Unlike the bpy complex, the primary product does not undergo any structural rearrangement and the photosubstitution preserves the *trans* configuration of the halide ligands.<sup>18</sup> Surprisingly, the TRIR experiment has uncovered [Ru(Cl)<sub>2</sub>(CO)<sub>2</sub>(iPr-dab)] as the first case of a slow CO dissociation from a thermally equilibrated triplet charge-transfer excited state, which takes place with a quantum yield of unity.

## Experimental Section

**Materials.** [Ru(SnPh<sub>3</sub>)(Cl)(CO)<sub>2</sub>(iPr-dab)],<sup>27</sup> [Ru(CH<sub>3</sub>)(I)(CO)<sub>2</sub>(iPr-dab)],<sup>25,28</sup> [Ru(I)<sub>2</sub>(CO)<sub>2</sub>(iPr-dab)],<sup>28</sup> and [Ru(Cl)<sub>2</sub>(CO)<sub>2</sub>(iPr-dab)]<sup>29</sup> were prepared according to published procedures and characterized by comparing their FTIR and <sup>1</sup>H NMR spectra with literature data.

**Time-Resolved IR Spectroscopy (TRIR).** TRIR measurements used the equipment described in detail previously.<sup>30–32</sup> In short, the sample solution was excited (pumped) at 400 nm, using frequency-doubled pulses from a Ti:sapphire laser of ~150 fs duration (fwhm). TRIR spectra were probed with IR (~150 fs) pulses obtained by difference-frequency generation, which cover a spectral range ca. 200 cm<sup>-1</sup> wide. Pumping with 355 nm, 1 ns pulses and electronic control of the time delay between the pump and probe pulses were used in the nanosecond range.<sup>32</sup> The pump and probe laser beams were focused to a spot of a maximum diameter of 200 μm. About 30 mL of sample solutions in CH<sub>3</sub>CN was flowed through a CaF<sub>2</sub> IR cell, which was continuously moved in a raster pattern in two dimensions to minimize sample photolysis. Optical path lengths of 0.5–1 mm were used. The sample concentration was adjusted to achieve an IR absorbance in the ν(CO) region of about 0.3. All spectral and kinetic fitting procedures were performed using Microcal Origin 7.1 software.

**Quantum Chemical Calculations.** The ground-state electronic structures were calculated by density functional theory (DFT)

- (9) Aarnts, M. P.; Stufkens, D. J.; Wilms, M. P.; Baerends, E. J.; Vlček, A., Jr.; Clark, I. P.; George, M. W.; Turner, J. J. *Chem.—Eur. J.* **1996**, *2*, 1556.
- (10) Kleverlaan, C. J.; Stufkens, D. J. *J. Photochem. Photobiol. A* **1998**, *116*, 109.
- (11) Nieuwenhuis, H. A.; van de Ven, M. C. E.; Stufkens, D. J.; Oskam, A.; Goubitz, K. *Organometallics* **1995**, *14*, 780.
- (12) Eskelinen, E.; Kinnunen, T.-J. J.; Haukka, M.; Pakkanen, T. A. *Eur. J. Inorg. Chem.* **2002**, 1169.
- (13) Eskelinen, E.; Haukka, M.; Venäläinen, T.; Pakkanen, T. A.; Wasberg, M.; Chardon-Noblat, S.; Deronzier, A. *Organometallics* **2000**, *19*, 163.
- (14) Luukkainen, S.; Haukka, M.; Eskelinen, E.; Pakkanen, T. A.; Lehtovuori, V.; Kallioinen, J.; Myllyperkiö, P.; Korppi-Tommola, J. E. I. *Phys. Chem. Chem. Phys.* **2001**, *3*, 1992.
- (15) Gabriëlsson, A.; Zálíš, S.; Matousek, P.; Towrie, M.; Vlček, A., Jr. *Inorg. Chem.* **2004**, *43*, 7380.
- (16) Haukka, M.; Kiviaho, J.; Ahlgrén, M.; Pakkanen, T. A. *Organometallics* **1995**, *14*, 825.
- (17) Chardon-Noblat, S.; Deronzier, A.; Ziessel, R.; Zsoldos, D. *Inorg. Chem.* **1997**, *36*, 5384.
- (18) Breuer, J.; Frühauf, H.-W.; Smeets, W. J. J.; Spek, A. L. *Inorg. Chim. Acta* **1999**, *291*, 438–447.
- (19) Vlček, A., Jr. *Coord. Chem. Rev.* **2002**, *230*, 225.
- (20) Sato, S.; Sekine, A.; Ohashi, Y.; Ishitani, O.; Blanco-Rodríguez, A. M.; Vlček, A., Jr.; Unno, T.; Koike, K. *Inorg. Chem.* **2007**, *46*, 3531.
- (21) Collomb-Dunand-Sauthier, M.-N.; Deronzier, A.; Ziessel, R. *J. Organomet. Chem.* **1993**, *444*, 191.
- (22) Lehtovuori, V.; Kallioinen, J.; Myllyperkiö, P.; Haukka, M.; Korppi-Tommola, J. *Chem. Phys.* **2003**, *295*, 81.
- (23) Lehtovuori, V.; Aumanen, J.; Myllyperkiö, P.; Rini, M.; Nibbering, E. T. J.; Korppi-Tommola, J. *J. Phys. Chem. A* **2004**, *108*, 1644.
- (24) Lehtovuori, V.; Myllyperkiö, P.; Linnanto, J.; Manzoni, C.; Polli, D.; Cerullo, G.; Haukka, M.; Korppi-Tommola, J. *J. Phys. Chem. B* **2005**, *109*, 17538.
- (25) Rohde, W.; Tom Dieck, H. J. *Organomet. Chem.* **1987**, *328*, 209.
- (26) Kleverlaan, C. J.; Stufkens, D. J.; Fraanje, J.; Goubitz, K. *Eur. J. Inorg. Chem.* **1998**, 1243.

- (27) Aarnts, M. P.; Stufkens, D. J.; Oskam, A.; Fraanje, J.; Goubitz, K. *Inorg. Chim. Acta* **1997**, *256*, 93.
- (28) Kraakman, M. J. A.; Vrieze, K.; Kooijman, H.; Spek, A. L. *Organometallics* **1992**, *11*, 3760.
- (29) de Klerk-Engels, B.; Frühauf, H.-W.; Vrieze, K.; Kooijman, H.; Spek, A. L. *Inorg. Chem.* **1993**, *32*, 5528.
- (30) Towrie, M.; Grills, D. C.; Dyer, J.; Weinstein, J. A.; Matousek, P.; Barton, R.; Bailey, P. D.; Subramaniam, N.; Kwok, W. M.; Ma, C. S.; Phillips, D.; Parker, A. W.; George, M. W. *Appl. Spectrosc.* **2003**, *57*, 367.
- (31) Vlček, A., Jr.; Farrell, I. R.; Liard, D. J.; Matousek, P.; Towrie, M.; Parker, A. W.; Grills, D. C.; George, M. W. *J. Chem. Soc., Dalton Trans.* **2002**, 701.
- (32) Towrie, M.; Parker, A. W.; Vlček, A., Jr.; Gabriëlsson, A.; Blanco Rodríguez, A. M. *Appl. Spectrosc.* **2005**, *59*, 467.

methods using *Gaussian 03*,<sup>33</sup> the Perdew, Burke, and Ernzerhof hybrid functional PBE0<sup>34</sup> with 25% HF exchange. Low-lying excited states were calculated by time-dependent DFT (TD-DFT). The geometry of the lowest-lying triplet state was optimized by an unrestricted Kohn–Sham calculation. Vibrational frequencies were calculated at optimized geometries corresponding to the functional and basis set used. The polarizable conductor calculation model (CPCM)<sup>35</sup> was used for modeling of the solvent influence. 6-311G\* polarized valence triple- $\zeta$  basis sets<sup>36,37</sup> (geometry optimization) or aug-cc-pvdz,<sup>38</sup> correlation-consistent polarized valence double- $\zeta$  basis sets augmented by diffuse functions (TD-DFT), were used for H, C, N, O, Cl, and I atoms. The quasi-relativistic effective core pseudopotentials and the corresponding optimized set of basis functions were employed for Ru.<sup>39</sup>

## Results

**Electronic Excited States.** The lowest electronic absorption band of the complexes  $[\text{Ru}(\text{X})(\text{X}')(\text{CO})_2(\text{iPr-dab})]$  has a maximum at 395 nm (X,X' = I,I),<sup>25</sup> 435 nm (SnPh<sub>3</sub>,Cl),<sup>9</sup> 463 nm (Me,I),<sup>6,9</sup> and 469 nm (Cl,Cl),<sup>40</sup> with one or two shoulders at slightly longer wavelengths. Irradiation at 400 nm, used in this study, excites predominantly the lowest allowed electronic transition, whose origin was intensively studied both experimentally and theoretically.<sup>2,9,40–44</sup> Previous results are confirmed and made more precise by present DFT and TD-DFT calculations that include the solvent and use the PBE0 functional (Tables S1–S8 and Figure S1 in the Supporting Information). The lowest allowed transition originates in a HOMO–1  $\rightarrow$  LUMO excitation whereby the electron density is transferred from the Ru(halide)(CO)<sub>2</sub> moiety to the iPr-dab ligand. Most of the transferred electron density originates at the Ru and halide atoms; these transitions are often denoted as MLCT/XLCT, where MLCT and

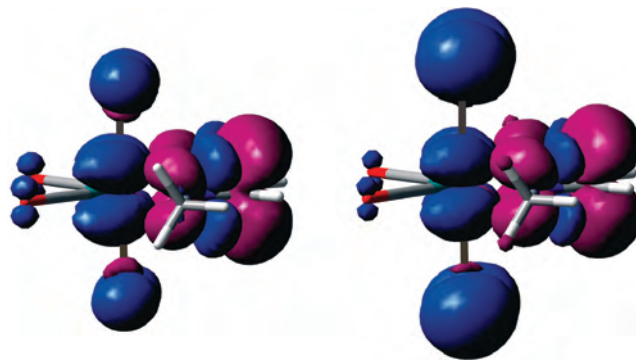


**Figure 2.** Electron-density difference between the lowest triplet excited state and the ground state of  $[\text{Ru}(\text{Cl})_2(\text{CO})_2(\text{Me-dab})]$  (left) and  $[\text{Ru}(\text{I})_2(\text{CO})_2(\text{Me-dab})]$  (right). Regions populated and depopulated upon excitation are shown in violet and blue, respectively.

XLCT stand for the  $\text{Ru}(d\pi) \rightarrow \text{dab}(\pi^*)$  and  $\text{X}(p\pi) \rightarrow \text{dab}(\pi^*)$  excitations, respectively. (Alternative abbreviations MLLCT (metal–ligand to ligand) and MLCT/LLCT are also used in the literature.) Mixing of MLCT and XLCT characters can be traced down to mixing of the Ru 4d( $\pi$ ) and halide p( $\pi$ ) orbitals in the depopulated HOMO–1. The XLCT contribution increases on going from the chloride to the iodide from  $\sim 54\%$  to  $\sim 79\%$ , as can be estimated from the HOMO–1 composition.

The lowest triplet state of  $[\text{Ru}(\text{Cl})_2(\text{CO})_2(\text{iPr-dab})]$  was calculated by TD-DFT at 2.45 eV and characterized as a mixed MLCT/XLCT/IL transition, where IL stands for an intraligand dab-localized  $\pi \rightarrow \pi^*$  excitation (Table S4 in the Supporting Information). This is best visualized by the difference electron-density map shown in Figure 2. The lowest triplet state of  $[\text{Ru}(\text{I})_2(\text{CO})_2(\text{iPr-dab})]$  has a similar mixed character (Figure 2, right). The XLCT contribution in the iodo complex is much larger at the expense of MLCT. Optimization of the triplet structures (Table S9 in the Supporting Information) and subsequent vibrational analysis yielded excited-state C $\equiv$ O stretching,  $\nu(\text{CO})$ , energies, which are in excellent agreement with experimental data (Table 1), validating the triplet DFT calculations.

**TRIR Spectra of  $[\text{Ru}(\text{SnPh}_3)(\text{Cl})(\text{CO})_2(\text{iPr-dab})]$ ,  $[\text{Ru}(\text{CH}_3)(\text{I})(\text{CO})_2(\text{iPr-dab})]$ , and  $[\text{Ru}(\text{I})_2(\text{CO})_2(\text{iPr-dab})]$ .** Ground-state FTIR spectra of these complexes show two strong bands due to symmetric ( $A_1$ ) and antisymmetric ( $B_1$ )  $\nu(\text{CO})$  vibrations, which occur higher and lower in frequency, respectively (Table 1). [The  $A_1$  and  $B_1$  labels assume the  $C_{2v}$  symmetry of the equatorial  $\text{Ru}(\text{CO})_2(\text{iPr-dab})$  moiety. This is strictly valid only for  $[\text{Ru}(\text{X})_2(\text{CO})_2(\text{iPr-dab})]$ , while  $A'$  and  $A''$  respectively would be more correct for  $[\text{Ru}(\text{SnPh}_3)(\text{Cl})(\text{CO})_2(\text{iPr-dab})]$  and  $[\text{Ru}(\text{CH}_3)(\text{I})(\text{CO})_2(\text{iPr-dab})]$ .] Ground-state  $\nu(\text{CO})$  energies are much higher for the dichloro and diiodo species  $[\text{Ru}(\text{X})_2(\text{CO})_2(\text{iPr-dab})]$  than for the mixed-ligand complexes. This is caused by strong  $\sigma$  donation (and, possibly, also by  $\pi$  donation through hyperconjugation) from the  $\text{CH}_3$  or  $\text{SnPh}_3$  ligands, which increases the electron density on the Ru and strengthens the  $\pi$  back-donation to CO.

- (33) Frisch, M. J.; Trucks, G. W.; Schlegel, H. B.; Scuseria, G. E.; Robb, M. A.; Cheeseman, J. R.; Montgomery, J. A.; Vreven, T.; Kudin, K. N.; Burant, J. C.; Millam, J. M.; Iyengar, S. S.; Tomasi, J.; Barone, V.; Mennucci, B.; Cossi, M.; Scalmani, G.; Rega, N.; Petersson, G. A.; Nakatsuji, H.; Hada, M.; Ehara, M.; Toyota, K.; Fukuda, R.; Hasegawa, J.; Ishida, M.; Nakajima, T.; Honda, Y.; Kitao, O.; Nakai, H.; Klene, M.; Li, X.; Knox, J. E.; Hratchian, H. P.; Cross, J. B.; Bakken, V.; Adamo, C.; Jaramillo, J.; Gomperts, R.; Stratmann, R. E.; Yazyev, O.; Austin, A. J.; Cammi, R.; Pomelli, C.; Ochterski, J. W.; Ayala, P. Y.; Morokuma, K.; Voth, G. A.; Salvador, P.; Dannenberg, J. J.; Zakrzewski, V. G.; Dapprich, S.; Daniels, A. D.; Strain, M. C.; Farkas, O.; Malick, D. K.; Rabuck, A. D.; Raghavachari, K.; Foresman, J. B.; Ortiz, J. V.; Cui, Q.; Baboul, A. G.; Clifford, S.; Cioslowski, J.; Stefanov, B. B.; Liu, G.; Liashenko, A.; Piskorz, P.; Komaromi, I.; Martin, R. L.; Fox, D. J.; Keith, T.; Al-Laham, M. A.; Peng, C. Y.; Nanayakkara, A.; Challacombe, M.; Gill, P. M. W.; Johnson, B.; Chen, W.; Wong, M. W.; Gonzalez, C.; Pople, J. A. *Gaussian 03*, revision C.02; Gaussian, Inc.: Wallingford, CT, 2004.
- (34) Perdew, J. P.; Burke, K.; Ernzerhof, M. *Phys. Rev. Lett.* **1996**, *77*, 3865.
- (35) Cossi, M.; Rega, N.; Scalmani, G.; Barone, V. *J. Comput. Chem.* **2003**, *24*, 669.
- (36) Glukhovtsev, M. N.; Pross, A.; McGrath, M. P.; Radom, L. *J. Chem. Phys.* **1995**, *103*, 1878.
- (37) Krishnan, R.; Binkley, J. S.; Seeger, R.; Pople, J. A. *J. Chem. Phys.* **1980**, *72*, 650.
- (38) Woon, D. E.; Dunning, T. H., Jr. *J. Chem. Phys.* **1995**, *103*, 4572.
- (39) Andrae, D.; Häussermann, U.; Dolg, M.; Stoll, H.; Preuss, H. *Theor. Chim. Acta* **1990**, *77*, 123.
- (40) Turki, M.; Daniel, C.; Zálíš, S.; Vlček, A., Jr.; van Slageren, J.; Stufkens, D. J. *J. Am. Chem. Soc.* **2001**, *123*, 11431.
- (41) Zálíš, S.; Ben Amor, N.; Daniel, C. *Inorg. Chem.* **2004**, *43*, 7978.
- (42) Vlček, A., Jr.; Zálíš, S. *Coord. Chem. Rev.* **2007**, *251*, 258.
- (43) Daniel, C. *Coord. Chem. Rev.* **2002**, *230*, 65.
- (44) Daniel, C. *Coord. Chem. Rev.* **2003**, *238–239*, 143.



**Table 1.**  $\nu(\text{CO})$  IR Bands of [Ru(X)(X')(CO)<sub>2</sub>(iPr-dab)] in the Ground State and the Lowest Triplet Excited State<sup>a</sup>

| complex   | ground state   |                | excited state     |                | $\Delta$         |                  | av $\Delta$ | diff $\Delta$ |
|---|----------------|----------------|-------------------|----------------|------------------|------------------|-------------|---------------|
|   | B <sub>1</sub> | A <sub>1</sub> | B <sub>1</sub>    | A <sub>1</sub> | B <sub>1</sub>   | A <sub>1</sub>   |             |               |
| [Ru(I) <sub>2</sub> (CO) <sub>2</sub> (iPr-dab)]                    | 1998           | 2054           | 2018              | 2072           | +20              | +18              | +19.0       | -2            |
| [Ru(I) <sub>2</sub> (CO) <sub>2</sub> (Me-dab)] calcd <sup>e</sup>  | 2001           | 2056           | 2033              | 2077           | +32              | +21              | +26.5       | -11           |
| [Ru(SnPh <sub>3</sub> )(Cl)(CO) <sub>2</sub> (iPr-dab)]             | 1973           | 2032           | 2003              | 2051           | +30 <sup>b</sup> | +19 <sup>b</sup> | +24.5       | -11           |
| [Ru(CH <sub>3</sub> )(I)(CO) <sub>2</sub> (iPr-dab)]                | 1966           | 2030           | 2011              | 2064           | +45 <sup>c</sup> | +34 <sup>c</sup> | +39.5       | -11           |
| [Ru(Cl) <sub>2</sub> (CO) <sub>2</sub> (iPr-dab)] exptl             | 2000           | 2062           | 2057 <sup>d</sup> | 2105           | +57              | +43              | +50         | -14           |
| [Ru(Cl) <sub>2</sub> (CO) <sub>2</sub> (Me-dab)] calcd <sup>e</sup> | 1999           | 2063           | 2053              | 2102           | +54              | +39              | +46.5       | -15           |
| [Ru(Cl) <sub>2</sub> (CH <sub>3</sub> CN)(CO)(iPr-dab)]             |                | 1969           |                   |                |                  |                  |             |               |

<sup>a</sup>  $\Delta$  = shift of the IR band upon excitation, av  $\Delta$  = average shift upon excitation =  $\frac{1}{2}(\Delta(A_1) + \Delta(B_1))$ , diff  $\Delta$  = change in the splitting between A<sub>1</sub> and B<sub>1</sub> upon excitation. All values are in cm<sup>-1</sup>. <sup>b</sup> Measured in CH<sub>2</sub>Cl<sub>2</sub>. Shifts of +30 and +17 cm<sup>-1</sup> were reported<sup>9</sup> from nanosecond TRIR, after excitation at 355 nm. <sup>c</sup> Shifts of +40 and +26 cm<sup>-1</sup> were determined<sup>7</sup> in CH<sub>2</sub>Cl<sub>2</sub> at 5 ns after excitation at 532 nm. <sup>d</sup> Estimated, the bleach and excited state bands strongly overlap. <sup>e</sup> UKS DFT G03/PBE0/CPCM (CH<sub>3</sub>CN), calculated values scaled by 0.9574.

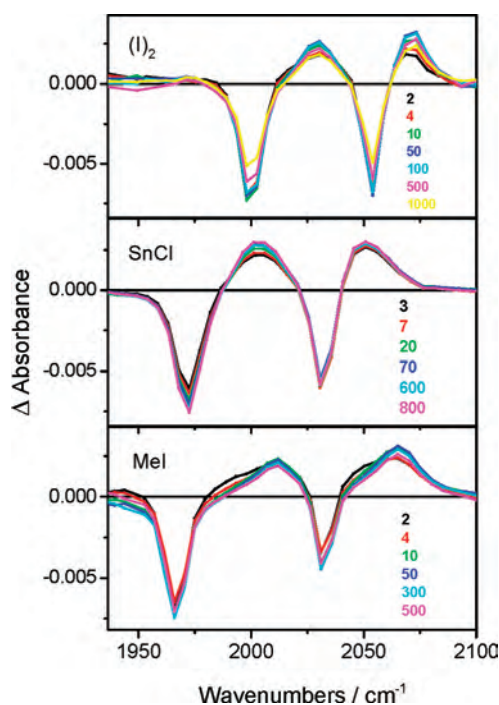


**Figure 3.** Difference TRIR spectra of [Ru(I)<sub>2</sub>(CO)<sub>2</sub>(iPr-dab)] in CH<sub>3</sub>CN (top), [Ru(SnPh<sub>3</sub>)(Cl)(CO)<sub>2</sub>(iPr-dab)] in CH<sub>2</sub>Cl<sub>2</sub> (middle), and [Ru(Me)(I)(CO)<sub>2</sub>(iPr-dab)] in CH<sub>3</sub>CN (bottom) measured at selected time delays in picoseconds after 400 nm excitation. Experimental points are separated by 4–5 cm<sup>-1</sup>.

Excitation produces within the 2 ps experimental time resolution two negative bleach bands, which are due to depletion of the ground-state population, and two positive excited-state bands at higher wavenumbers (Figure 3 and Table 1). Small dynamic shifts of the excited-state bands to higher energies and narrowing, which are apparent during the first 1–20 ps in the spectra of [Ru(SnPh<sub>3</sub>)(Cl)(CO)<sub>2</sub>(iPr-dab)] and [Ru(CH<sub>3</sub>)(I)(CO)<sub>2</sub>(iPr-dab)], manifest vibrational

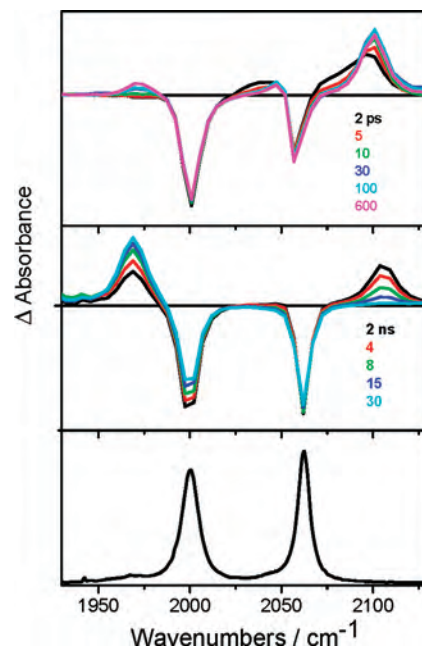


**Figure 4.** Difference TRIR spectra of [Ru(Cl)<sub>2</sub>(CO)<sub>2</sub>(iPr-dab)] in CH<sub>3</sub>CN. Top: picosecond spectra measured at selected time delays after 400 nm excitation. Bottom: nanosecond spectra measured at selected time delays after 355 nm excitation. Experimental points are separated by 4–5 cm<sup>-1</sup>.

relaxation and solvent cooling.<sup>45–47</sup> These effects are negligible for [Ru(I)<sub>2</sub>(CO)<sub>2</sub>(iPr-dab)]. Later, the spectra show neither any significant decay of the IR intensity nor a change in the  $\nu(\text{CO})$  spectral pattern until the end of the examined 1000 ps time window, indicating long excited-state lifetimes (Table 1).

**TRIR Spectra of [Ru(Cl)<sub>2</sub>(CO)<sub>2</sub>(iPr-dab)].** Excitation of [Ru(Cl)<sub>2</sub>(CO)<sub>2</sub>(iPr-dab)] in CH<sub>3</sub>CN produces two negative bleach bands at 2062 and 2000 cm<sup>-1</sup> due to depletion of the ground state and two broad positive bands at 2105 and ~2057 cm<sup>-1</sup>, which belong to the excited state (Figure 4). The latter band strongly overlaps with the bleach at 2062 cm<sup>-1</sup>, decreasing its relative intensity. The 2105 cm<sup>-1</sup> band undergoes a dynamic shift to higher wavenumbers by ~13 cm<sup>-1</sup> with a principal lifetime estimated as 2 ps, plus a smaller 11 ps contribution. This is caused by vibrational relaxation and solvent/solute cooling, respectively.<sup>45–47</sup> On a longer time scale, the intensity of both excited-state bands decreases, while a new band due to a photoproduct grows in at 1969 cm<sup>-1</sup>. This band is attributed to *cis*(CO, CH<sub>3</sub>CN), *trans*(Cl, Cl)-[Ru(Cl)<sub>2</sub>(CH<sub>3</sub>CN)(CO)(iPr-dab)], based on a close similarity with the spectra of analogous complexes *cis*(CO, MeOH), *cis*(Cl, Cl)-[Ru(Cl)<sub>2</sub>(MeOH)(CO)(bpy)] (1967 cm<sup>-1</sup>),<sup>18</sup> *cis*(CO, CH<sub>3</sub>CN), *trans*(I, I)-[Ru(I)<sub>2</sub>(CH<sub>3</sub>CN)(CO)(iPr-dab)] (1975 cm<sup>-1</sup>),<sup>25</sup> or polymeric [Ru(Cl)<sub>2</sub>(CO)(iPr-dab)]<sub>n</sub> (1972 cm<sup>-1</sup>).<sup>29</sup> The decay of the excited-state IR band at 2105 cm<sup>-1</sup> mirrors the rise of the photoproduct band at 1969 cm<sup>-1</sup> (Figure 5) occurring with a common lifetime of 7.2 ns.

(45) Liard, D. J.; Busby, M.; Matousek, P.; Towrie, M.; Vlček, A., Jr. *J. Phys. Chem. A* **2004**, *108*, 2363.

(46) Blanco-Rodríguez, A. M.; Busby, M.; Grădinaru, C.; Crane, B. R.; Di Bilio, A. J.; Matousek, P.; Towrie, M.; Leigh, B. S.; Richards, J. H.; Vlček, A., Jr.; Gray, H. B. *J. Am. Chem. Soc.* **2006**, *128*, 4365.

(47) Blanco-Rodríguez, A. M.; Ronayne, K. L.; Zálaiš, S.; Sýkora, J.; Hof, M.; Vlček, A., Jr. *J. Phys. Chem. A* **2008**, in press.

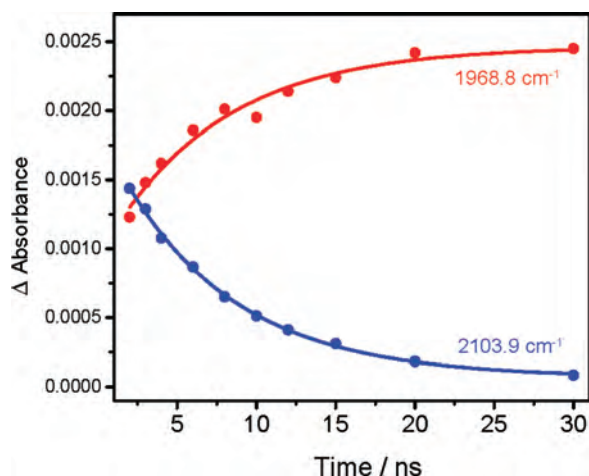


**Figure 5.** Time profiles of the maximum intensity of the excited-state (blue) and photoproduct (red) IR bands of  $[\text{Ru}(\text{Cl})_2(\text{CO})_2(\text{iPr-dab})]$  in  $\text{CH}_3\text{CN}$ . The curves correspond to single-exponential fits:  $7.2 \pm 0.3$  ns at  $2103.9$   $\text{cm}^{-1}$  and  $7.3 \pm 1.3$  ns at  $1968.8$   $\text{cm}^{-1}$ .

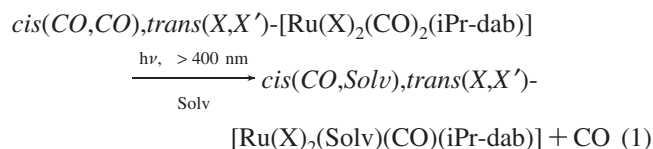
## Discussion

The TRIR experiments and DFT calculations presented above report on the character of the lowest excited states of the complexes  $[\text{Ru}(\text{X})(\text{X}')(\text{CO})_2(\text{iPr-dab})]$  and reveal a uniquely “slow” CO dissociation from a relaxed excited state. In all experiments, the studied photoprocesses were triggered by excitation at 400 nm, which is directed to the lowest allowed CT transition. As discussed above, this transition entails an extensive shift of the electron density from the  $\pi$  system of the Ru(halide)(CO)<sub>2</sub> moiety to the  $\pi^*$  orbital of the iPr-dab ligand (Figure S1 in the Supporting Information). Optical excitation is followed by intersystem crossing into the lowest triplet state, which is expected<sup>48,49</sup> to occur on a femtosecond time scale. The TRIR spectra measured from 2 ps onward thus report only on the behavior of the lowest triplet excited state.

Excited-state  $\nu(\text{CO})$  bands of  $[\text{Ru}(\text{X})(\text{X}')(\text{CO})_2(\text{iPr-dab})]$  are shifted to higher energies from their ground-state positions. This is typical for excited states with a  $\text{Ru}(\text{CO})_2 \rightarrow \text{dab}$  MLCT component,<sup>7,9,15,42,50–53</sup> which depopulates the CO  $\pi^*$  orbital, strengthening the C≡O bond. XLCT excitation affects the  $\nu(\text{CO})$  energies much less because it does not involve the  $\pi^*(\text{CO})$  orbitals directly. Contributions from intraligand  $\pi\pi^*$  excitation decrease the  $\nu(\text{CO})$  energies because of the diminishing  $\pi$ -acceptor strength of the dab ligand.<sup>54</sup> The magnitude of the  $\nu(\text{CO})$  shift upon excitation increases depending on the ligands X,X' in the order  $(\text{I})_2 < (\text{Sn})(\text{Cl}) < (\text{Me})(\text{I}) < (\text{Cl})_2$ , which reflects the increasing

contribution of the MLCT excitation to the lowest excited state. It can be concluded that the lowest triplet excited state has a mixed MLCT/XLCT character, where the relative contribution of the MLCT and XLCT excitations strongly depends on the ligands. Indeed, DFT calculations clearly demonstrate the decreasing XLCT and increasing MLCT contributions on going from  $[\text{Ru}(\text{I})_2(\text{CO})_2(\text{iPr-dab})]$  to  $[\text{Ru}(\text{Cl})_2(\text{CO})_2(\text{iPr-dab})]$  (Figure 2). The  $\nu(\text{CO})$  energies of excited  $[\text{Ru}(\text{Cl})_2(\text{CO})_2(\text{iPr-dab})]$  are very high even in absolute terms, indicating that the  $\text{Ru} \rightarrow \text{CO}$   $\pi$  back-donation is very weak. The difference between the excited-state  $\nu(\text{CO})$  bands, which is related to the CO–CO interaction force constant,<sup>55</sup> is much smaller for  $[\text{Ru}(\text{I})_2(\text{CO})_2(\text{iPr-dab})]$  than the other three complexes. TRIR spectra also show that the vibrational and solvent relaxation (i.e., thermal equilibration) is completed within a few tens of picoseconds, at most.

The complexes  $[\text{Ru}(\text{SnPh}_3)(\text{Cl})(\text{CO})_2(\text{iPr-dab})]$  and  $[\text{Ru}(\text{CH}_3)(\text{I})(\text{CO})_2(\text{iPr-dab})]$  are stable under continuous irradiation<sup>5,6,8–11,26</sup> with excited-state lifetimes<sup>6,9</sup> of 700 and 127 ns, respectively. Accordingly, the TRIR spectra show only the two bands of the <sup>3</sup>MLCT/XLCT states, which do not decrease in intensity during the first 1 ns. Both dihalide complexes  $[\text{Ru}(\text{X})_2(\text{CO})_2(\text{iPr-dab})]$  (X = Cl, I) were reported to undergo photochemical substitution of one CO ligand by a solvent molecule, which occurs with retention of the configuration (eq 1).<sup>18,25</sup>



In the case of  $[\text{Ru}(\text{I})_2(\text{CO})_2(\text{iPr-dab})]$ , TRIR spectra measured up to 1 ns do not provide evidence for photoproduct formation, except for an extremely weak absorption feature at  $\sim 1972$   $\text{cm}^{-1}$ , which can be seen from about 10 ps onward and stays constant until the end of the time interval investigated, 1 ns. No mechanistic conclusions can be drawn from the present experiments. On the other hand, TRIR spectra of  $[\text{Ru}(\text{Cl})_2(\text{CO})_2(\text{iPr-dab})]$  clearly show direct conversion of the <sup>3</sup>MLCT/XLCT excited state into the  $[\text{Ru}(\text{Cl})_2(\text{CH}_3\text{CN})(\text{CO})(\text{iPr-dab})]$  photoproduct, which occurs with a 7.2 ns lifetime, with no observable intermediates. The absence of any ground-state recovery suggests that the initial quantum yield is (nearly) unity. This behavior indicates a predominantly dissociative or I<sub>d</sub> interchange mechanism, where the primary product is very rapidly ( $\ll 7$  ns) stabilized by solvent coordination.

Photochemistry of  $[\text{Ru}(\text{Cl})_2(\text{CO})_2(\text{iPr-dab})]$  presents a special case of a “slow” CO photosubstitution from a relaxed <sup>3</sup>MLCT excited state. This is a remarkable reaction indeed, considering that CO photodissociation from carbonyldiimine complexes in most cases occurs from optically excited singlet MLCT states with femtosecond rates.<sup>15,19,20,31,56–59</sup> Even the

(48) Cannizzo, A.; van Mourik, F.; Gawelda, W.; Zgrabcic, G.; Bressler, C.; Chergui, M. *Angew. Chem., Int. Ed.* **2006**, *45*, 3174.

(49) Cannizzo, A.; Blanco-Rodríguez, A. M.; Nahhas, A.; Šebera, J.; Zálíš, S.; Vlček, A., Jr.; Chergui, M. *J. Am. Chem. Soc.* **2008**, in press.

(50) Schoonover, J. R.; Strouse, G. F. *Chem. Rev.* **1998**, *98*, 1335.

(51) George, M. W.; Turner, J. J. *Coord. Chem. Rev.* **1998**, *177*, 201.

(52) Kuimova, M. K.; Alsindi, W. Z.; Dyer, J.; Grills, D. C.; Jina, O. S.; Matousek, P.; Parker, A. W.; Portius, P.; Sun, X.-Z.; Towrie, M.; Wilson, C.; Yang, J.; George, M. W. *Dalton Trans.* **2003**, 3996.

(53) Dattelbaum, D. M.; Omberg, K. M.; Schoonover, J. R.; Martin, R. L.; Meyer, T. J. *Inorg. Chem.* **2002**, *41*, 6071.

(54) Dattelbaum, D. M.; Omberg, K. M.; Hay, P. J.; Gebhart, N. L.; Martin, R. L.; Schoonover, J. R.; Meyer, T. J. *J. Phys. Chem. A* **2004**, *108*, 3527.

(55) Cotton, F. A.; Kraihanzel, C. S. *J. Am. Chem. Soc.* **1962**, *84*, 4432.

(56) Vlček, A., Jr. *Coord. Chem. Rev.* **1998**, *177*, 219.

(57) Víchová, J.; Hartl, F.; Vlček, A., Jr. *J. Am. Chem. Soc.* **1992**, *114*, 10903.

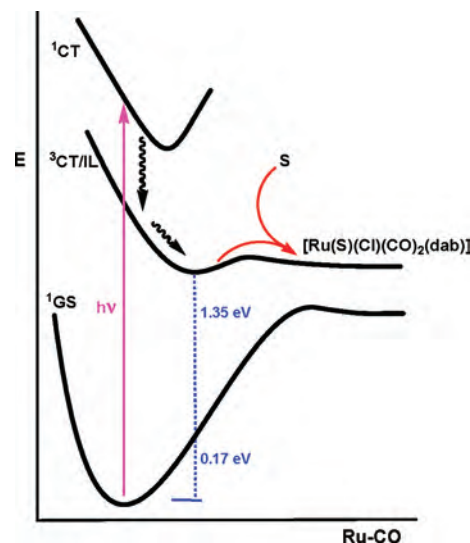
closely related [Ru(Cl)<sub>2</sub>(CO)<sub>2</sub>(bpy)] loses CO from its <sup>1</sup>MLCT/XLCT excited state on a subpicosecond time scale.<sup>15,23,24</sup> Triplet MLCT or MLCT/XLCT states of carbonyldiimine complexes are usually unreactive, and their population provides an efficient deactivation pathway to the ground state, preventing any further CO dissociation. Such “trapping” triplet CT states have been described in detail<sup>15,58</sup> for [Cr(CO)<sub>4</sub>(bpy)] or [Ru(I)<sub>2</sub>(CO)<sub>2</sub>(bpy)]. The only reactive <sup>3</sup>MLCT states are known for [M(CO)<sub>4</sub>(diimine)] (M = W or Mo), which undergo CO substitution by an associative mechanism.<sup>19,60–62</sup> However, this reaction requires the presence of strong nucleophiles in high concentrations and occurs with very low quantum yields, at most 0.04, measured for [Mo(CO)<sub>4</sub>(1,10-phenanthroline)].<sup>60–62</sup>

To understand the slow dissociative CO photosubstitution in [Ru(Cl)<sub>2</sub>(CO)<sub>2</sub>(iPr-dab)], we need to ask why the optically prepared <sup>1</sup>MLCT/XLCT state is unreactive and what the origin of the triplet-state reactivity is. Singlet MLCT and XLCT states gain their photoreactivity through interaction with higher-lying, usually ligand-field [i.e., d(π) → d(σ\*)] or M → CO MLCT excited states, which are dissociative with respect to the M–CO bond.<sup>15,19,56,59,63–67</sup> Avoided crossing, which occurs along the M–CO reaction coordinate, then mixes the dissociative state with the optically populated singlet CT state, changing its electronic parentage and the shape of the potential energy surface. The UV–vis absorption spectrum<sup>40</sup> and excited-state calculations of [Ru(Cl)<sub>2</sub>(CO)<sub>2</sub>(iPr-dab)] show that its lowest allowed <sup>1</sup>MLCT/XLCT transition is relatively isolated in energy. Moreover, close-lying higher states mostly involve excitations to π\*(dab) or Cl–Ru–Cl σ\* orbitals. Such states are not expected to be dissociative and interact with <sup>1</sup>MLCT/XLCT at longer Ru–CO distances. Instead of bond breaking, the optically populated <sup>1</sup>MLCT/XLCT state undergoes intersystem crossing to the lowest triplet state <sup>3</sup>MLCT/XLCT.

The CO dissociation from the relaxed <sup>3</sup>MLCT/XLCT state of [Ru(Cl)<sub>2</sub>(CO)<sub>2</sub>(iPr-dab)] can be explained in two ways, which can be discriminated upon by considering the energetics and structural changes upon excitation:

(a) The energetic minimum of the <sup>3</sup>MLCT/XLCT state lies above the energy barrier of the ground-state Ru–CO dissociation. The reaction occurs by intersystem crossing from <sup>3</sup>MLCT/XLCT onto the ground-state surface through a conical intersection, followed by fast CO dissociation. This possibility can be clearly excluded by the energetics: The

**Scheme 1.** Proposed Model of Excited-State Dynamics and Photochemistry of [Ru(Cl)<sub>2</sub>(CO)<sub>2</sub>(iPr-dab)]<sup>a</sup>



<sup>a</sup> The wavy arrows denote intersystem crossing and triplet-state relaxation. S stands for a solvent molecule from the first solvation sphere.

energy of the relaxed triplet was calculated as 1.52 eV above the ground-state minimum (=E<sub>00</sub>) and 1.35 eV vertically above the ground-state potential energy surface. The difference between these values, 0.17 eV, is clearly much smaller than the Ru–CO bond dissociation energy, estimated to be at least 1 eV. The excited-state minimum thus lies above the strongly bound region of the ground-state potential energy surface, and intersystem crossing to the ground state would simply restore the original geometry (Scheme 1).

(b) Instead, we propose that the CO loss is caused by the electron deficiency of the Ru center and a weakening of Ru–CO bonds in the excited state. The high ν(CO) frequencies show that the electron density on Ru is rather low already in the ground state. TRIR shows a very large increase of ν(CO) upon triplet excitation, which manifests further weakening of the Ru → CO π back-donation and a decrease of the electron density at the Ru(CO)<sub>2</sub> moiety, which becomes susceptible to attack by neighboring solvent molecule(s). Calculated elongation of Ru–CO bonds upon excitation to the lowest triplet by 0.082 Å (Table S9 in the Supporting Information) indicates weakening of Ru–CO bonds and easier steric accessibility for the incoming solvent molecule. As a result, the potential energy surface of the lowest triplet state along the Ru–CO dissociation coordinate is only weakly bound because of a small dissociation energy and a gradually strengthening interaction with a solvent molecule during the reaction (Scheme 1).

## Conclusions

[Ru(Cl)<sub>2</sub>(CO)<sub>2</sub>(iPr-dab)] presents the first case of a kinetically characterized “slow” (7.2 ns) photochemical CO dissociation from a thermally relaxed <sup>3</sup>MLCT/XLCT excited state, which acts as an excitation energy reservoir. Excitation activates the complex both thermodynamically, by increasing the energy above the dissociation limit, and kinetically, by

- (58) Farrell, I. R.; Matousek, P.; Towrie, M.; Parker, A. W.; Grills, D. C.; George, M. W.; Vlček, A., Jr. *Inorg. Chem.* **2002**, *17*, 4318.  
 (59) Farrell, I. R.; Vlček, A., Jr. *Coord. Chem. Rev.* **2000**, *208*, 87.  
 (60) Wieland, S.; Reddy, K. B.; van Eldik, R. *Organometallics* **1990**, *9*, 1802.  
 (61) Fu, W.-F.; van Eldik, R. *Inorg. Chem.* **1998**, *37*, 1044.  
 (62) Fu, W.-F.; van Eldik, R. *Organometallics* **1997**, *16*, 572.  
 (63) Vlček, A., Jr.; Víchová, J.; Hartl, F. *Coord. Chem. Rev.* **1994**, *132*, 167.  
 (64) Guillaumont, D.; Daniel, C.; Vlček, A., Jr. *J. Phys. Chem. A* **2001**, *105*, 1107.  
 (65) Pollak, C.; Rosa, A.; Baerends, E. J. *J. Am. Chem. Soc.* **1997**, *119*, 7324.  
 (66) Baerends, E. J.; Rosa, A. *Coord. Chem. Rev.* **1998**, *177*, 97.  
 (67) Goumans, T. P. M.; Ehlers, A. W.; van Hemert, M. C.; Rosa, A.; Baerends, E. J.; Lammertsma, K. *J. Am. Chem. Soc.* **2003**, *125*, 3558.



weakening the Ru–CO bond and making the Ru atom susceptible to solvent coordination by electronic depopulation and by increasing its sterical accessibility.

The lowest triplet state of [Ru(X)(X')(CO)<sub>2</sub>(iPr-dab)] (X = X' = Cl or I; X = Me, X' = I; X = SnPh<sub>3</sub>, X' = Cl) has a mixed MLCT/XLCT character. The XLCT contribution is much larger for the iodo than the chloro complexes. For the bishalide complexes, the lowest triplet also contains a significant admixture of an intraligand  $\pi\pi^*(\text{dab})$  character. The intraligand admixture is absent for the lowest two singlets.

DFT and TD-DFT calculations model very well the low-lying singlet electronic excited states and the lowest triplet state of this class of complexes, provided that the solvent is

included in the calculation. Triplet UKS-DFT calculation predicts the excited-state IR spectra with a good accuracy.

**Acknowledgment.** Funding and support from EPSRC, the COST Action D35, STFC Rutherford Appleton Laboratory, QMUL, Ministry of Education of the Czech Republic (Grant 1P05OC68), and the Grant Agency of the Academy of Sciences of the Czech Republic (Grant KAN100400702) are gratefully acknowledged.

**Supporting Information Available:** Tables S1–S9, Figure S1, and additional references. This material is available free of charge via the Internet at <http://pubs.acs.org>.

IC702304K